TABLE OF CONTENTS (Continued)

CHAPTER I

INTRODUCTION

(i)

(ii)

Fig. 1.

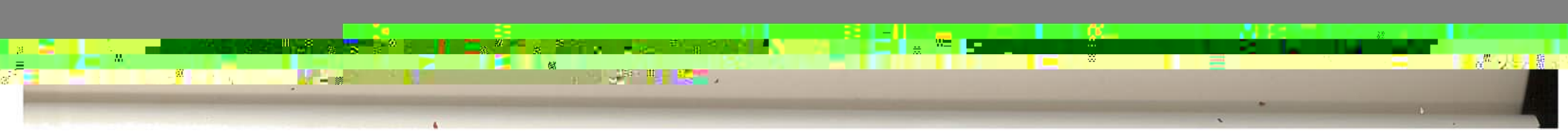

Fig. 2. Division of a unit sphere into "directional mesh" (only upper section for S_4 quadrature shown)

$\Omega \rightarrow \Omega$

$$\mu_o = \text{Cos}\theta = \hat{\Omega}' \cdot \quad - - - - -$$

wher

is t

Fig. 5. Division of the whole energy range into several energy intervals

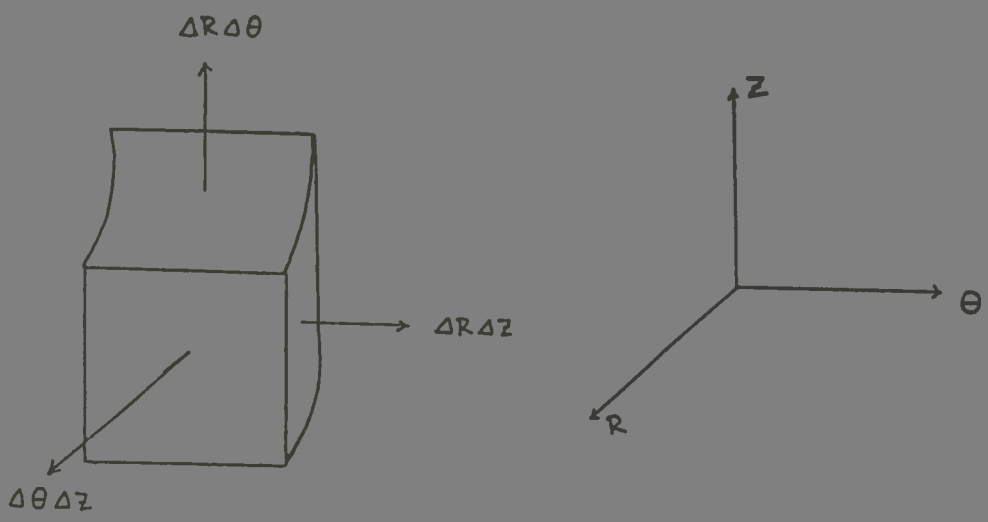

volume = $\Delta R \Delta \theta \Delta z$

$A^V =$ $V =$

$2\pi R(\Delta Z)$ $2\pi \bar{R} \Delta R(\Delta Z)$

$2\pi R(\Delta \theta)$ ΔR $2\pi \bar{R} \Delta R(\Delta \theta)$

Fig. 6b. Two-dimensional mesh cells for R-Z and R-θ geometries

$$\int_{Z_L} \Phi_{RZ} dZ \quad - \quad (32)$$

where Z_L and Z_U are the lower and upper limits of integration. In this case, the axial limits Z_L and Z_U should be large enough so that

$$\int_{Z_L}^{Z_U} \Phi_{RZ} dZ \cong \int_{-\infty}^{+\infty} \Phi_{RZ} dZ \quad - \quad (33)$$

This approximation follows directly from Equation (26). Unfortunately, this approximation usually underestimates the radial channel fluxes, because the R-Z channel flux falls off slowly in the Z direction, consequently preventing expression (33) from being very accurate unless Z_U and Z_L are very large. Often the upper and lower Z values used in R-Z channel flux calculation do not satisfy this condition.

2. Synthesis Approximation in R-Θ-Z System of Coordinates

We now define the synthesized 3-D flux as a function of R,Θ,Z variables for the cylindrical geometry to be[8]

$$\Phi_{sg}(R,\Theta,Z) \simeq \frac{\Phi_g(R,Z) * \Phi_g(R,\Theta)}{\Phi_g(R)} \quad - - - - - - - - - - - - - - - - - \quad (34)$$

where, $\Phi_{sg}(R,\Theta,Z) \equiv$ multigroup synthesized 3-D flux.

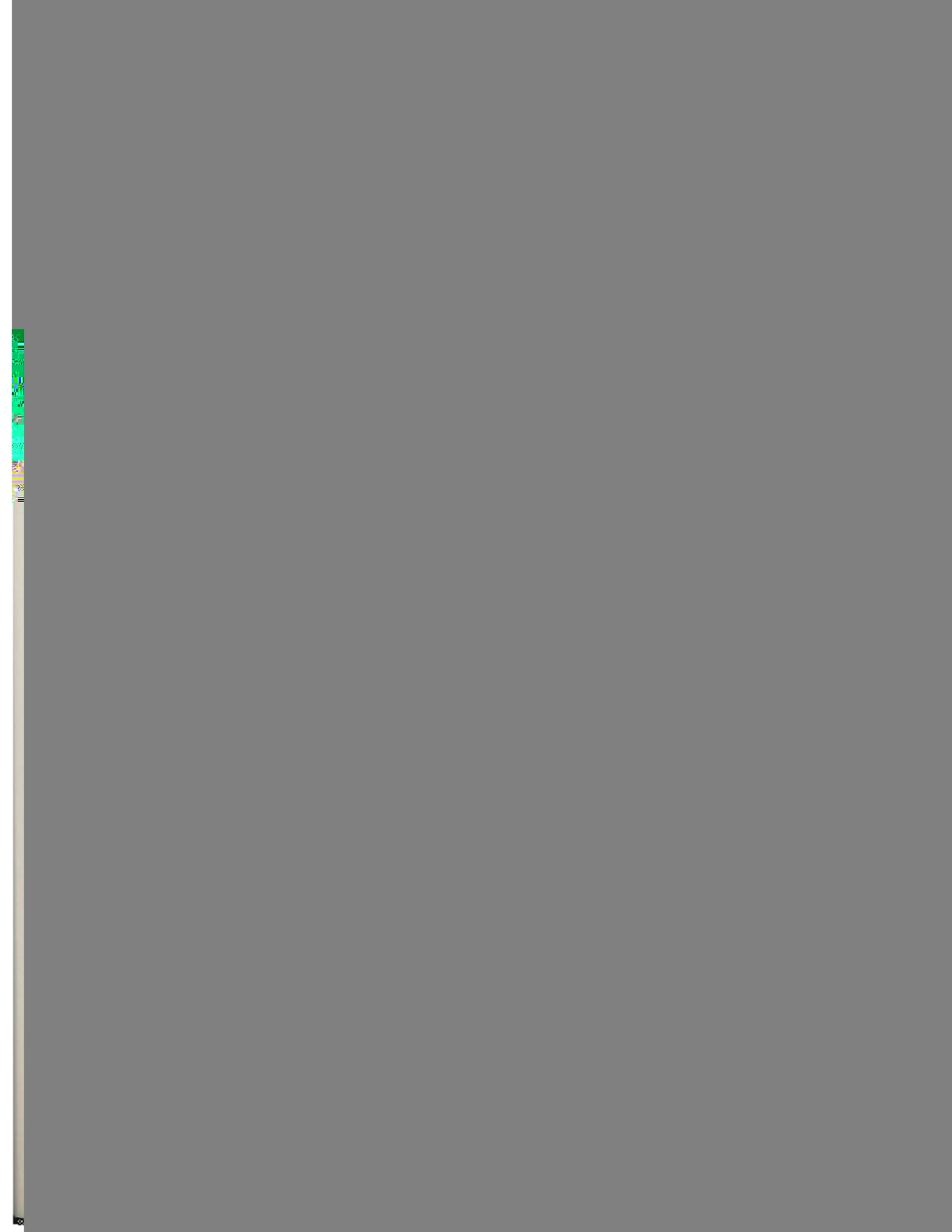

Fig. 8. Sequence of Calculations in DOTSYN

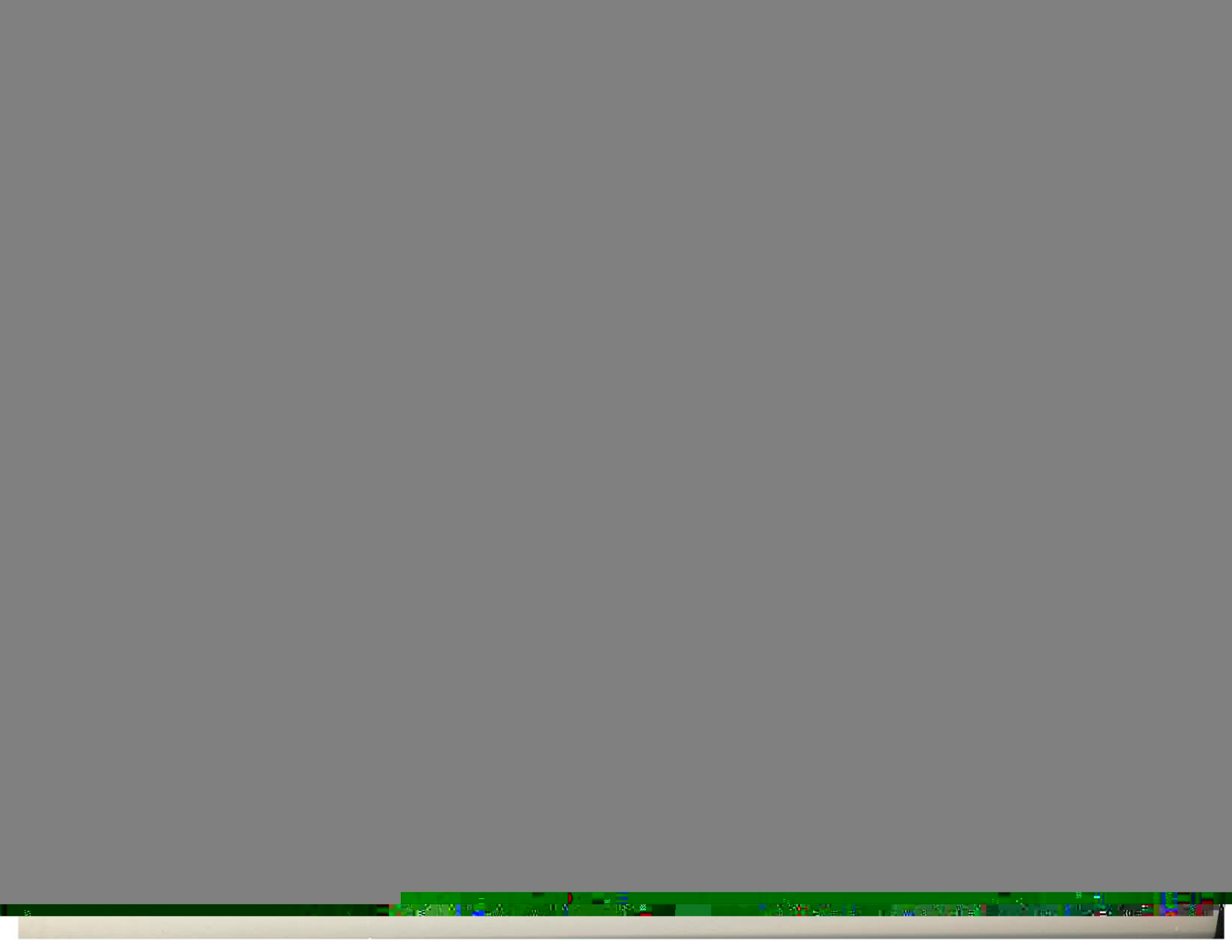

A. Model Configurations of the Reactor

The cross-sectional view of the reactor vessel and internals of the ANO-1 nuclear reactor is shown in fig. 9, and fig. 10 shows the vertical cross section of this reactor.

The configuration consists of 177 fuel assemblies in the core, which is surrounded by a 1.91-cm-thick stainless steel baffle. A stainless steel core barrel of inner diameter 358.14 cm surrounds the baffle. Outside the core barrel is a stainless steel thermal shield. There are four surveillance specimen holder tubes attached to the outer side of the thermal shield. Water flows downward through the downcomer region

Fig. 9. Cross-sectional view of ANO-1 nuclear reactor

Fig. 10. Cut-away view of ANO-1 showing the pressure vessel and other components

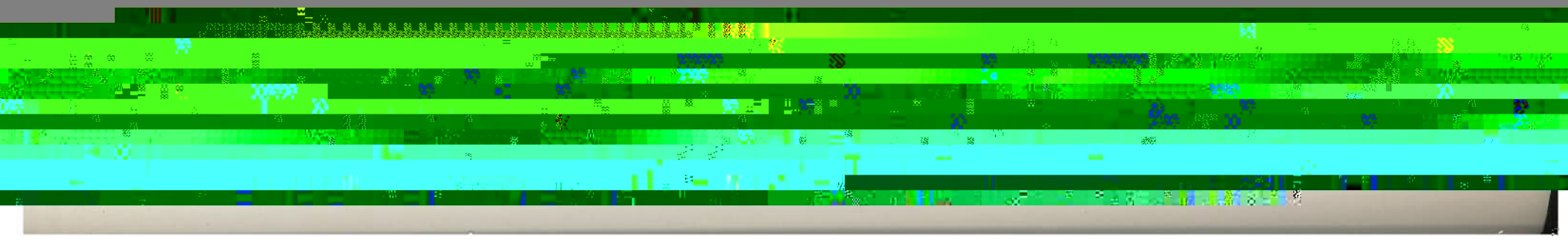

TABLE 1 (continued)

	49,734
	171,470
	534,440
	83.39
	5.66
	17.63
	654
	1280
eg. F	4220
	131.32×10^6
	49.19
	15.73
	647.1
	1.78
	1.70
	3.03
	97.3

Fig. 12.

ND.
D.


6.00
(C)

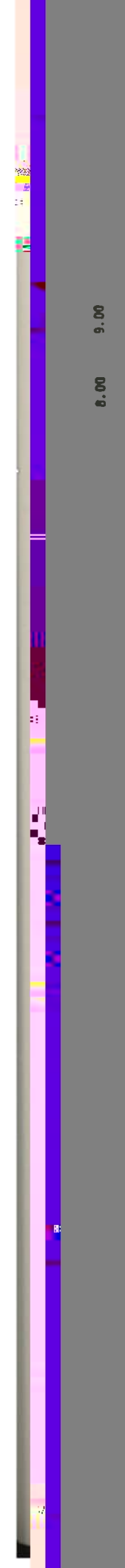

Fig. 16. R-Z view of ANO-1 up to pressure vessel (along R) and nozzle top (along Z). Zones are shown by numbers. scale: 1.0 cm = 34.455 cm

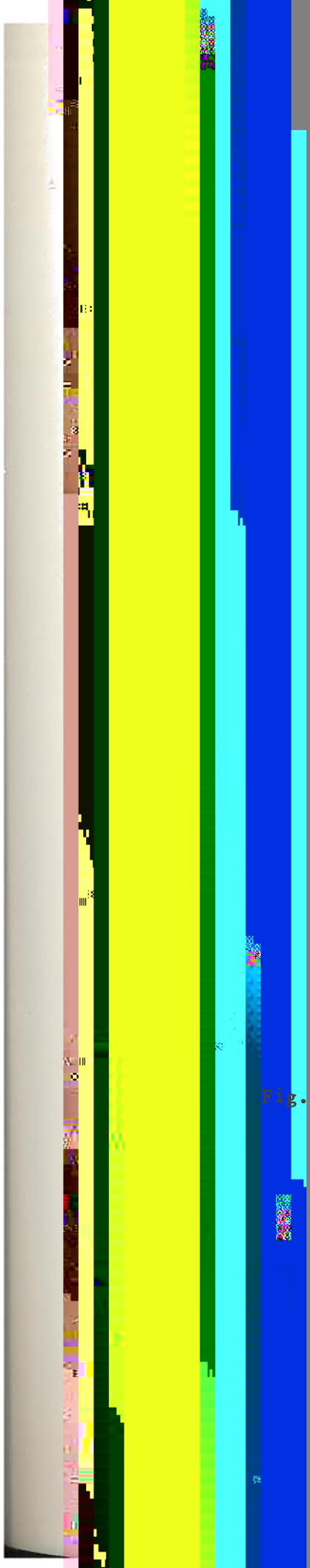

Fig. 18. 1-D model (with meshes) of ANO-1 up to RPV (along R).
scale: 1.0 cm = 34.455 cm

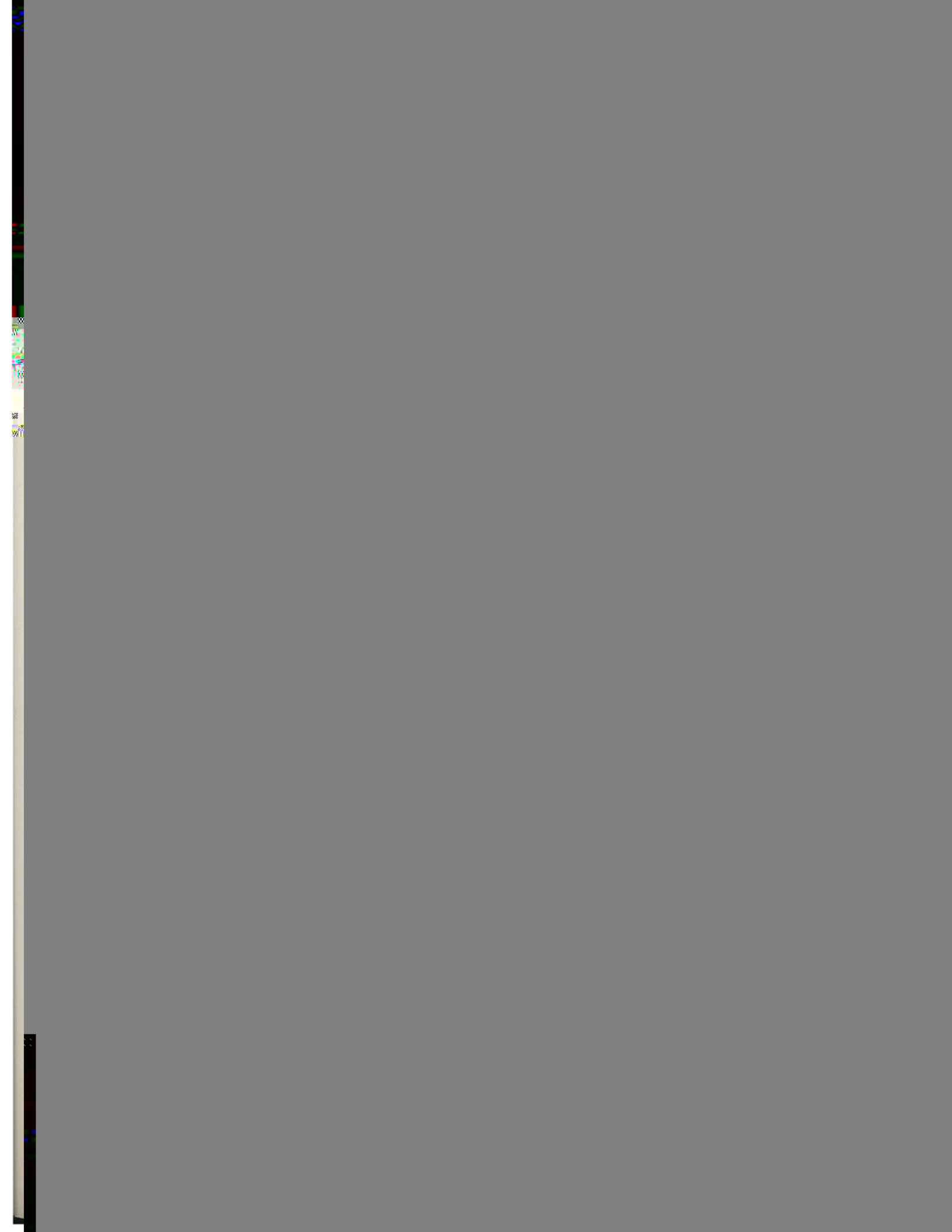

TABLE 4

Materials and Their Atom Densities[4]
Zones of the 3-D and 2-D Models

TABLE 6

Comparison of Total Flux by TORT and DOTSYN at the Peak Flux Location (θ = 9°) at the 1/4T of the Pressure Vessel

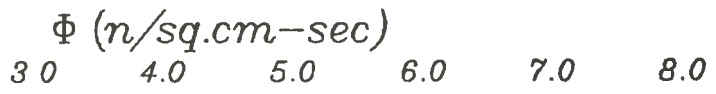
Φ (n/sq.cm–sec)
3.0
4.0
5.0
6.0
7.0
8.0

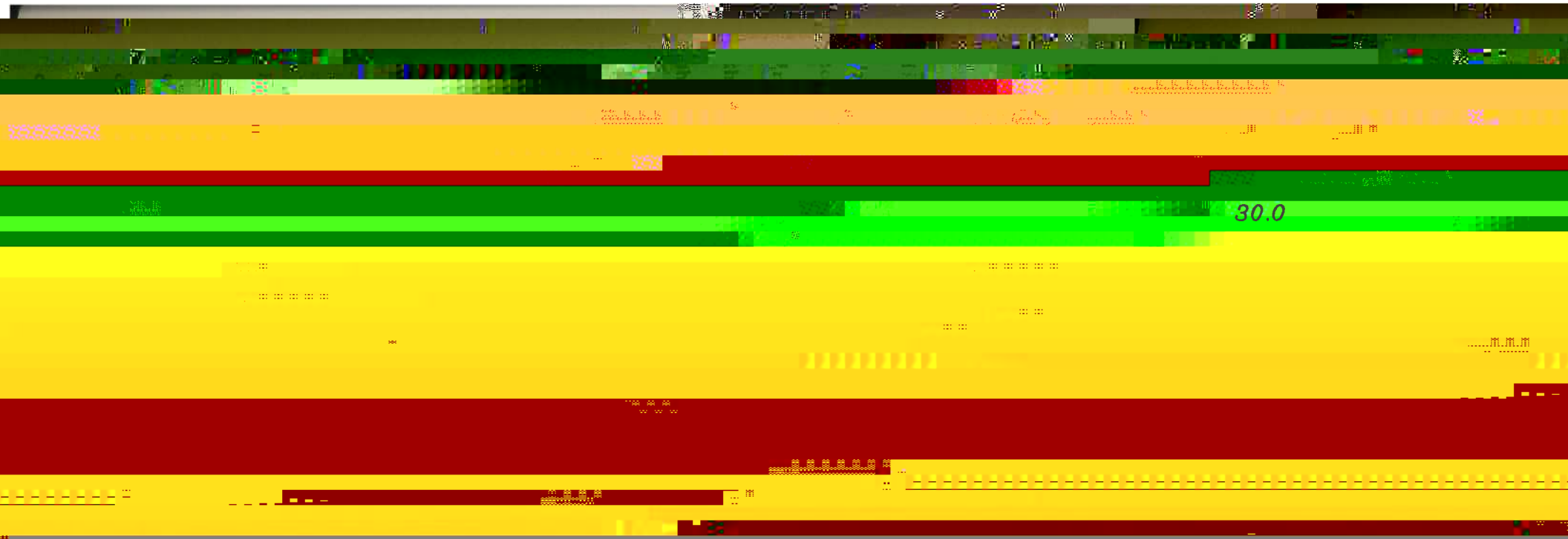
30.0

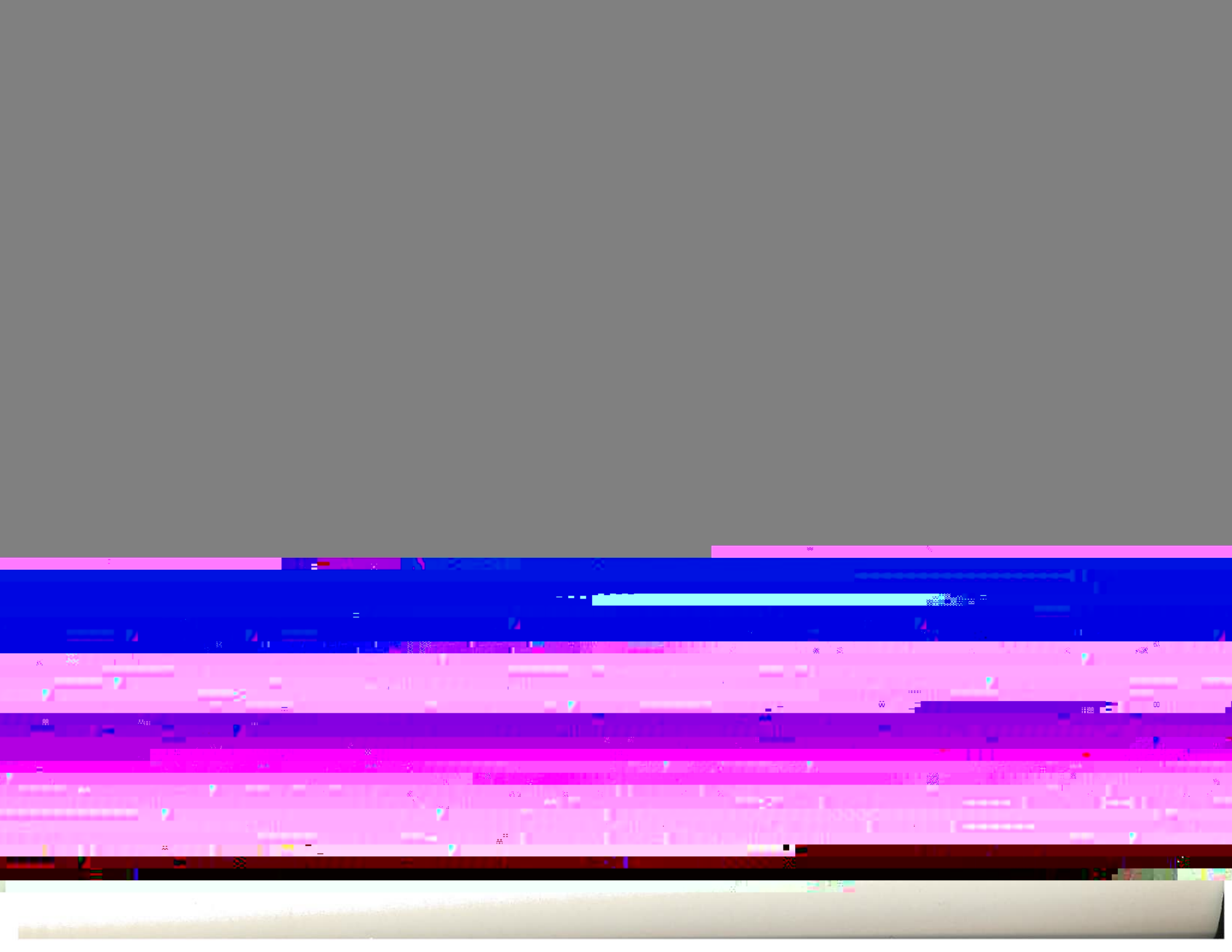

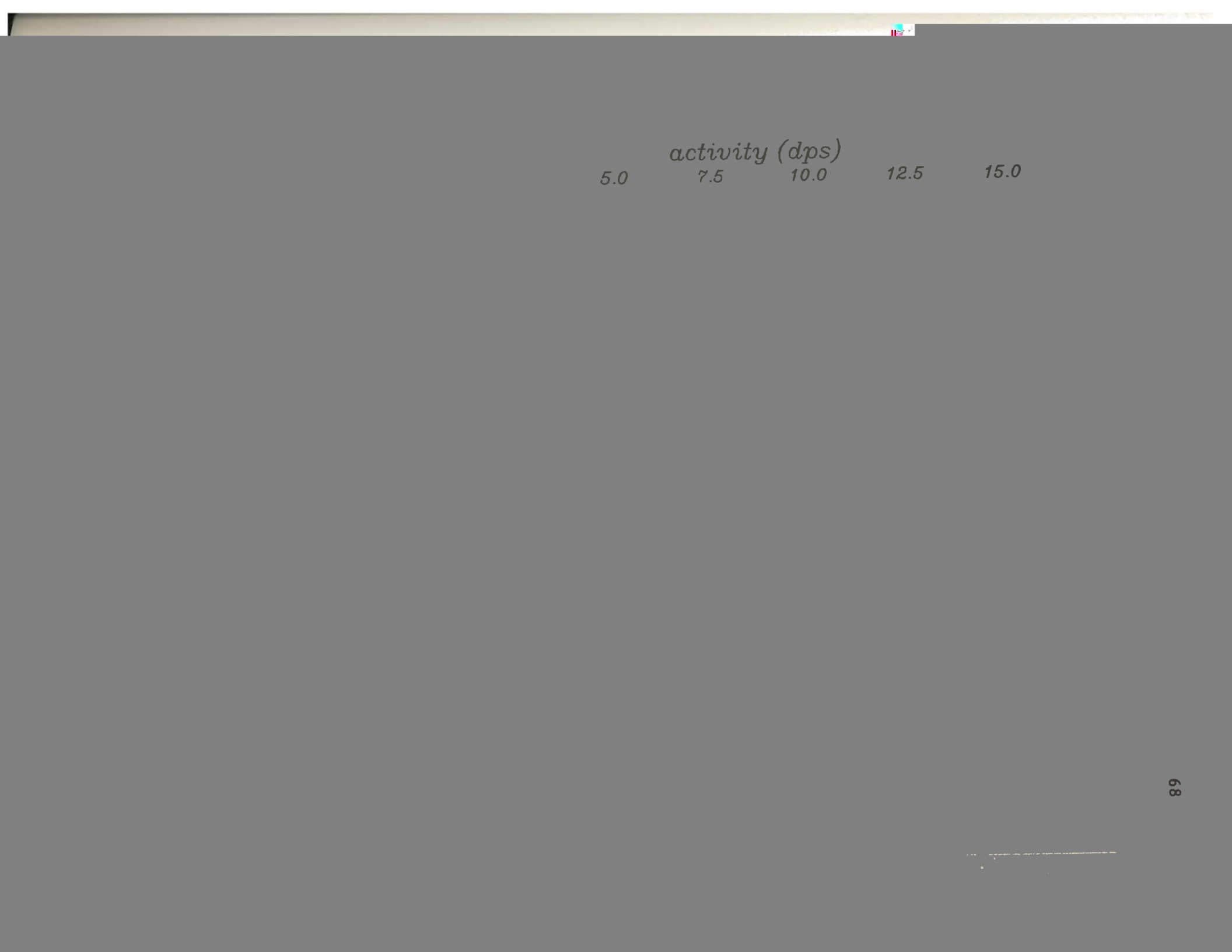
activity (dps)
5.0
7.5
10.0
12.5
15.0

act

activity (dps)
2.0
3.0
4.0
5.0
6.0
7.0
8.0

□ =
○ =

Φ (*n/sq cm sec*)

14.0
12.0
10.0
2.0